Method to Recover Connate Water From Reservoir Cores Using Centrifuge and Surfactant-Enhanced oil for Formation Evaluation

Hussain Al Qatari[1], *Shouxiang* Ma[2], *Taha* Okashah[1], and *Najebah M.* Alsaleh[1]

[1]Hallibuton Energy Services, Research & Development Department, 31952 Dhahran, Saudi Arabia
[2]Saudi Aramco, Reservoir Description & Simulation Department, Saudi Aramco, 31311 Dhahran, Saudi Arabia

Abstract. In formation evaluation, reservoir initial water saturation (S_{wi}) is commonly calculated using resistivity-based Archie equation, which requires inputs of formation water resistivity (R_w). As S_{wi} in reservoir intervals is deemed capillary-bound irreducible, it is challenging to directly sampling S_{wi}, whether downhole formation fluid sampling or from laboratory oil-base-mud (OBM) cored samples. Consequently, R_w in S_{wi} calculations is often taken from the water leg below the hydrocarbon zone, assuming water properties are the same across both zones, which often is not appropriate. This study introduces a laboratory approach that enables partial recovery of S_{wi} from reservoir samples cored with bland OBM using centrifuge and surfactant-enhanced (SE) oil. The methodology is based on the principle that SE oil has significantly lower interfacial tension (IFT) with water, as compared to crude oil, allowing partial recovery of S_{wi}, especially when an applied centrifuge force is higher than the reservoir capillary pressure that binds S_{wi}. To demonstrate, outcrop cores are cleaned and 100% saturated with synthetic brine of known salinities. S_{wi} is then established using centrifuge and crude oil, mimicking oil migration, followed by aging for wettability restoration. Subsequently, the cores are centrifuged with SE oil, which has an oil-water IFT more than 10 times lower than that crude oil-water IFT, at a higher centrifuge speed. In this study, sandstone and carbonate cores are used. Mixing 2% surfactant by volume with oil lowered the IFT by 93% and 83% between oil and brines of 200 & 100 KPPM, respectively. This enabled recovery of 19–52% of the original S_{wi} for the carbonate samples and 29–35% for the sandstone samples. The developed procedures including measurement calibration and sample dilution allowed reliable geochemical assessment, by using methods titration and Ion Chromatography, of recovered S_{wi} despite its small volume, resolving a formation evaluation challenge in characterizing connate water salinity.

1 Introduction

The determination of water saturation (S_w) in the reservoir is a routine measurement because it is a critical indicator that influences decisions across drilling, well completion, and reservoir management. Thus, estimation of initial water saturation (S_{wi}), often called connate water saturation or irreducible water saturation in engineering terms (S_{wir}), is essential for reservoir characterization, field development, and optimizing oil recovery processes [1,2] as it directly influences reserve estimation, fluid flow modeling, and enhanced oil recovery assessment.

Obtaining S_{wi} is often based on resistivity logs, where core data is not only required [3-5], but also measured fit-for-purposely [6]. In doing so, the Archie Eq [7]

$$S_w^n = \frac{R_w}{R_t}\frac{1}{\emptyset^m} \quad (1)$$

for the drainage process should be written as

$$S_{w,dr}^{ndr} = \frac{R_{w,dr}}{R_{t,dr}}\frac{1}{\emptyset^m} \quad (2)$$

and for imbibition [8]

$$S_{w,imb}^{nimb} = \frac{R_{w,imb}}{R_t,imb}\frac{1}{\emptyset^m} \quad (3)$$

Where dr and imb indicate the process of drainage and imbibition, representing resistivity hysteresis [9,10].

In using Eqs 2 and 3 for formation evaluation and reservoir saturation monitoring, saturation exponents ndr and nimb can be determined from laboratory measurements [6]. Formation resistivities $R_{t,dr}$ and $R_{t,imb}$ can be obtained from running resistivity logs; openhole [11] or casedhole [8]. The challenge is to determine $R_{w,dr}$ and $R_{w,imb}$, which require proper characterization of formation water salinity.

Comparing to $R_{w,dr}$, determining $R_{w,imb}$ is relatively easier, with techniques ranging from the first order of approximation of taking formation water samples [8], to direct formation water salinity estimation by using such as pulsed neutron logging [12-15], formation dielectric logging with/without temperature transient analyses [16-19], spontaneous potential [20], or even through inversion of borehole produced water salinity measurement [21].

Determination of $R_{w,dr}$ has been and remains to be a challenge, because S_{wi} is often described as capillary bound and its mobility is extremely low, the reason why it is often called irreducible water, thus sampling S_{wi} is difficult. Although the mobility of S_{wi} is low, but it is not zero. Field examples of logs with shallow depth of

* Corresponding author: hussain.alqatari@halliburton.com

investigation have shown that S_{wi} may be reduced if oil-based mud (OBM) is used; attributed to the reduction of interfacial tension (IFT) between S_{wi} and the invading OBM filtrate [22] and/or alteration of reservoir wettability due to OBM filtrate invasion [23]. Laboratory studies have shown that the reduction of S_{wi} can be enhanced if the OBM can be designed with the maximum IFT reduction [24], then the reduced amount of S_{wi} may be analyzed in the laboratory for its salinity determination so that $R_{w,dr}$ can be properly estimated, resolving a challenge in routine formation evaluation.

The main objective of this paper is to study details about chemicals used to maximize IFT reduction, partial recovery of S_{wi}, and especially characterizing the often small amount of S_{wi} recovered for its salinity, as part of reservoir core cleaning for wettability restoration [25, 26].

2 Experimentation

2.1 Materials

2.1.1 Rock samples

In this study, a total of six outcrop core plugs were used; three Indiana Limestone and three Berea Sandstone. The carbonate plugs were coded as C-1 to C-3 and the Sandstone plugs as S-1 to S-3. Table 1 summarizes the petrophysical properties of the samples, with porosity ranged from 17% to 21% and permeability from 20 mD to 200 mD.

Table 1. Rock properties and brine salinity.

Plug ID	V_P (cc)	ρ_g (g/cc)	ϕ (%)	K (mD)	Brine Salinity (KPPM)
C-1	9.32	2.71	17.38	28.33	200
C-2	9.39	2.75	18.61	30.71	100
C-3	9.64	2.74	18.61	29.06	100
S-1	11.29	2.66	20.68	196.82	200
S-2	11.41	2.66	20.88	154.82	200
S-3	10.89	2.65	19.92	190.10	100

2.1.2 Fluids

The fluids used in this study are:

- Dead crude oil with density of 0.846 g/cc and viscosity of 6.227 cP @ room temperature.
- Oil soluble surfactant was mixed with the crude oil to make surfactant enhanced (SE) oil to reduce IFT [27].
- Two synthetic Sodium Chloride (NaCl) brines were prepared (Table 1) with concentrations of 100 and 200 KPPM to mimic high and intermediate formation connate water salinity.

2.2 Apparatus

2.2.1 Density and viscosity meter

Density and viscosity measurements of crude oil, 2% SE oil and brines were conducted using Anton Paar density-viscosity meter (model SVM 2001). Measuring viscosity and density at temperatures is essential for better handling the requirements of oil, brine, and understanding their flow behavior during flow experiments. Those properties also affect IFT between oil and brine [28]. Moreover, fluids densities are used to calculate the optimum speed to establish S_{wi} using a centrifuge [29]. Table 2 summarizes fluid density and viscosity measurements at room temperature of 22.3°C and high temperature of 70°C.

Table 2. Viscosity and density measurements of used fluids.

Measurement	Crude oil	2% SE Oil	200 KPPM Brine	100 KPPM Brine
ρ @22°C (g/cc)	0.846	0.848	1.129	1.065
ρ @70°C (g/cc)	0.806	0.804	1.067	1.014
μ @22°C (cP)	6.227	6.39	1.679	1.127
μ @ 70°C (cP)	2.19	2.15	0.74	0.55

2.2.2 Interfacial Tension (IFT) apparatus

Water-oil IFT was measured using a high temperature and high pressure (HTHP) pendent drop instrument (Temco Pendent Drop IFT cell), as shown in Figure 1. It consists of IFT cell, hand pump for injection of oil or water using a two way valve, vibration free table, needles, imaging system (video camera with computer display, monitor, software data storage and IFT calculation), temperature control system (water bath), lamp, transfer cells, and pressure transducers with digital display.

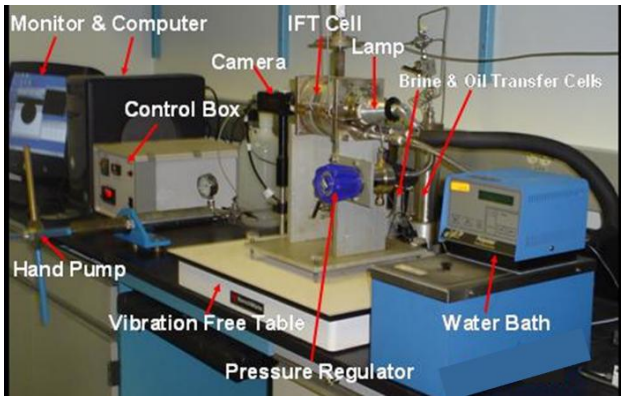

Figure 1. Pendent/rising drop interfacial tension system.

Recent progress in image analysis and data acquisition systems has made it possible to obtain a direct digitization of the drop image with the aid of a video frame grabber from the digital camera. The imaging and image analysis module was DROP image program which has a number of features that make the procedure of IFT measurements simpler and versatile.

IFT between crude oil and brine is commonly measured using rising drop method so the medium (brine) allows the light to go through and the camera captures the

oil drop shape. It provides accurate results under reservoir like conditions. With this technique, a small droplet of crude oil is formed at the needle tip located at the bottom of the chamber which is filled with brine at HPHT. The droplet forms a shape controlled by the balance between bouncy and interfacial forces, where a high-resolution camera captures its profile. The density of the tested fluids is required as part of the IFT calculations of the two phases. Specialized software analyzes the curvature of the drop to calculate the IFT [30]. This method was used to measure the IFT between the brines (the external phase) and crude oil & SE oil, as exampled by Figure 2.

Figure 2. Measuring IFT with a rising droplet of oil in brine.

2.2.3 Centrifuge

A high-speed centrifuge (Resifuge-RSS, Figure 3) was used in this study to establish core sample S_{wi} and also producing part of S_{wi}. Core samples were first saturated 100% with the assigned brine. To illustrate the concept that part of S_{wi} is recoverable, the optimum speed to establish the desired S_{wi} was estimated based on the dimensionless bond number (Nb) that is based on the centrifuge set up of rotor arm length from the center, samples length, permeability, fluids density and IFT. Consequently, samples with similar rock properties were placed in the centrifuge to perform the drainage test with crude oil till achieving the desired S_{wi}. A secondary drainage test was then performed at higher speed with SE oil for the partial recovery of the S_{wi}. Table 3 shows the speeds used and their associated capillary pressure for each sample.

Table 3. Calculated capillary pressure with each speed.

Plug ID	Speed 1 (RPM)	Pc (psi)	Speed 2 (RPM)	Pc (psi)
C-1	6500	57.45	8000	87.69
C-2	6500	44.01	8000	67.30
C-3	6500	44.88	8000	68.64
S-1	3000	12.19	4500	27.64
S-2	3000	12.19	4500	27.65
S-3	3000	9.78	4500	22.21

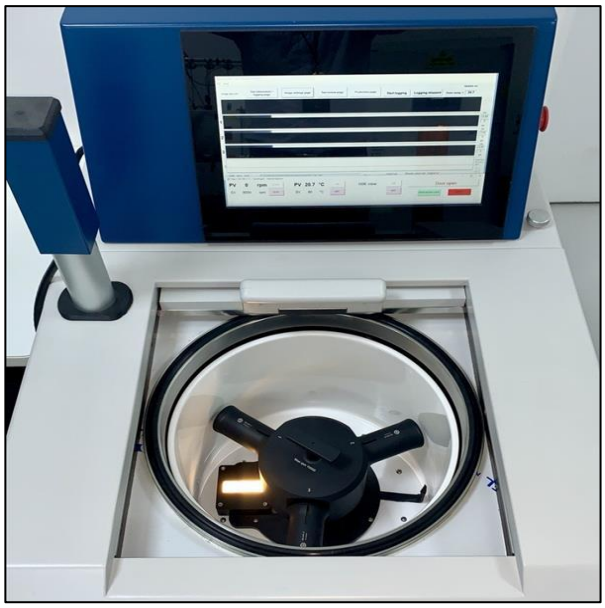

Figure 3. High speed centrifuge.

2.2.4 Geochemical analysis

To characterize the salinity of the produced brine, two methods were used; the titration method and the method of using an ion chromatography.

The Titration Method. This method is used to determine the concentration of NaCl in brine follows Mohr's method using titration with 0.1 N Silver Nitrate ($AgNO_3$), or SN, and Potassium Chromate (K_2CrO_4), or PC, as an indicator. The method is especially useful if the testing brine sample volume is small, such as ranging from 0.1 cc to 1 cc.

The method is based on the principle that SN reacts with Cl^- in the brine sample to form silver chloride (AgCl), a white precipitate. After all Cl^- is precipitated, further addition of SN reacts with chromate ions to form silver chromate (Ag_2CrO_4), a reddish-brown precipitate, which marks the endpoint of the titration process.

To conduct the titration test, the following are basic steps:

1. Use a calibrated micropipette to transfer the small volume of brine, 0.5 cc to 1 cc, to a clean 250 cc flask.
2. Add 100 cc distilled water to the flask.
3. Add 0.5 – 1 cc of 5% PC to the flask, solution appears pale yellow.
4. Fill a 50 cc burette with 0.1 N SN, record the initial volume accurately by ±0.01 cc.
5. Place the flask on a white background and begin titration while swirling.
6. Add SN to the flask, rapidly at the beginning, then very slowly near the endpoint.
7. Endpoint is reached when a faint, permanent reddish-brown color appears and persists after swirling for about 30 seconds.

The concentration of the NaCl, C_{NaCl}, in wt%, is then calculated from the volume and normality of the used SN:

$$C_{NaCl} = \frac{58.44 V_{SN} N_{SN}}{V_w} \quad (4)$$

Where:
V_w = Volume of brine sample (mL),
V_{SN} = Volume of SN ($AgNO_3$) used (mL),
N_{SN} = Normality of SN, around 0.1, but the exact value needs to be determined in the laboratory with known NaCl solution, for accuracy, and
58.44 = Molecular weight of NaCl (g/mol)

The method (Eq. 4) is valuable for small volume brine geochemical analysis, as is the case for trying to recover part of S_{wi}, an already small value.

The Ion Chromatography method. This method uses an Ion Chromatography (IC), for example Metrohm 940 Professional IC Vario which can take a minimum sample volume of about 0.3 cc, to determine the NaCl concentration in the brine by measuring the concentration of Cl ions. It is applicable for Cl concentration of brine samples where the dilution is required to lower the Cl levels within the instrument calibration range. It separates anions in aqueous solution using an ion exchange column. The Cl ion is quantified based on its retention time and peak area. Chloride standards are first analyzed to generate the calibration curve after the brine sample is injected and the Cl peak identified and quantified. The Cl concentration is then measured and converted to equivalent NaCl concentration using the molar mass relationship below:

$$C_{NaCl} = \frac{58.44}{35.45} C_{Cl-} = 1.647 C_{Cl-} \quad (5)$$

Where:
35.45 = Molecular weight of Cl^- (g/mol)
58.44 = Molecular weight of NaCl (g/mol)
C_{Cl^-} = Chloride concentration (PPM)
C_{NaCl} = Sodium Chloride concentration (PPM)

Calibration. To ensure measurement accuracy, calibrations are established by comparing the measurement with known input values. To achieve that, NaCl brine samples were prepared with concentrations ranging from 50, 100, 150 and 200 KPPM and the measurements were conducted by using both titration and IC methods. The NaCl concentrations were cross-plotted; Figures 4 and 5 for the titration and IC methods, respectively.

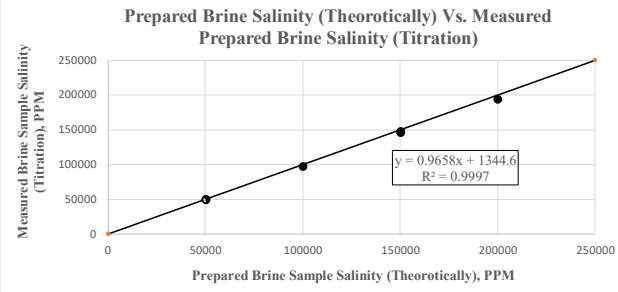

Figure 4. NaCl brine concentration cross plot between prepared and measured by using the titration method.

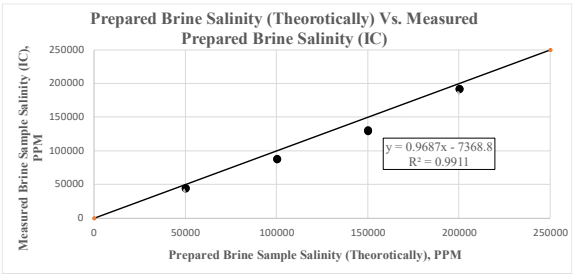

Figure 5. NaCl brine concentration cross plot between prepared and measured by using the IC method.

IC versus titration method. The IC method provides higher accuracy and reproducibility, as chloride is quantified instrumentally using a calibration curve and standards. This contrasts with the conventional titration method, which relies on a visual endpoint that may vary between operators, introducing subjective error. However, the IC method has several limitations, including the requirement for instrument calibration, sample dilution to fit within the calibration range, and increased operational complexity. In contrast, the titration method is simpler and faster to perform manually, but it is more susceptible to human error and variability associated with endpoint detection.

3 Experimental Procedures

To recover part of S_{wi} using a centrifuge and SE oil, the following experimental procedures were followed:

1) Six outcrop plugs of permeability greater than 15 mD were selected covering different mineralogy; three carbonate and three clastic samples.
2) All samples were washed after trimming and placed in an over at 105°C for drying until constant weight.
3) Porosity, permeability, and grain density [31] were measured (Table 1).
4) Samples were characterized by XRD & XRF for mineralogy and elemental analysis [32, 33] using plug end pieces.
5) CT scanning was performed to evaluate sample heterogeneity and integrity.
6) A crude oil was filtered using 5 microns filter and used for the establishment of the S_{wi} and aging for wettability restoration [25].
7) Oil soluble surfactant was selected to lower the IFT between the flooding oil and connate brine.
8) Brines with 200 and 100 KPPM NaCl were prepared, to mimic formation connate water of different concentrations.
9) Geochemical analysis of the prepared 200 and 100 KPPM NaCl brines was performed as a reference for calibration.
10) Density and viscosity of the crude oil, SE oil and brines were measured at room and high temperatures.
11) IFT was measured between:
    a) Crude oil and 200 KPPM NaCl brine.
    b) Crude oil and 100 KPPM NaCl brine.
    c) 1% SE Oil and 200 KPPM NaCl brine.
    d) 1% SE Oil and 100 KPPM NaCl brine.
    e) 2% SE Oil and 200 KPPM NaCl brine.

f) 2% SE Oil and 100 KPPM NaCl brine.

12) Both carbonate and clastic plugs were fully saturated with the assigned brines (Table 1).
13) Samples were then flooded by crude oil using the centrifuge to establish S_{wi} at the assigned speed (RPM 1); the primary drainage.
14) Once the S_{wi} was established, samples were put in the static aging cells filled with crude oil under 70°C and 1500 psi for 1 month to restore the wettability. Care was taken during this process by preparing the aging cells ahead and filling them with the crude oil. The samples were removed from the centrifuge, measured weight and then directly placed in the aging cell. More crude oil was pumped into the aging cells to raise the cells pressure before placing them in the aging oven at 70°C.
15) Samples were then extracted from the aging cells and flooded again by using the centrifuge but this time using 2% SE oil and at a higher speed (RPM 2) to recover part of the S_{wi}. Increasing the speed is an established method for recovering part of the S_{wi}. RPM 2 selected has enough higher Pc (Table 3) to accomplish this recovery without going at a much higher speed that may risk the samples in terms of mechanical failure [34].
16) Geochemical analysis of the collected volumes, often small depending on rock properties, of the brines recovered and compared with initial Geochemical analysis (Step 9) to assess the results and its representation.

4 Results and discussion

4.1 Rock sample XRD mineralogy

XRD analysis (Table 4) of the carbonate samples showed that the major mineral is calcite, about 93% to 94%. While the predominant mineral in the clastic samples is Quartz, from 75-77% with some clay minerals (13% to 15%) and feldspars (5% to 7%).

Table 4. XRD mineralogy results of samples

Minerals	Mineralogy of Core Samples (5)					
	C-1	C-2	C-3	S-1	S-2	S-3
Quartz	2.3	1.4	1.0	**77.1**	**75.1**	**74.8**
Feldspars	0.9	0.8	0.5	6.6	7.3	5.6
Clays	1.3	2.1	2.4	**13.3**	**14.7**	**14.4**
Pyrite	0.4	0.1	0.3	0.1	0.1	0.1
Calcite	**93.2**	**94.0**	**94.2**	0.9	1.1	0.5
Dolomite	0.1	0.1	0.1	0.2	-	0.1
Anhy-drite	0.3	0.2	0.1	0.2	0.1	0.2
Others	1.5	1.3	1.4	1.6	1.6	4.3

4.2 Rock sample CT scan images

The mechanical integrity of the rock samples is important to endure a laboratory test [34]. To confirm that the selected samples are free of internal fractures and that samples have similar internal pore structure, X-Ray computed tomography (CT) scanner was used to scan the samples at two different energies (Dual Energy) with high resolution of 0.5 mm along the plugs. The CT images have been processed to calculate bulk density (RhoB) and Photoelectric factor (PE) of each sample. The results of average RhoB and PE of each sample are presented in Table 5. Figures 6 and 7 show white light photos and processed CT images of the selected samples that confirm they are suitable for further testing in terms of mechanical integrity and homogeneity.

Table 5. Average bulk density and PE mineralogy of the samples at resolution of 0.5 mm.

Plug ID	CT RhoB (g/cc)	CT PE (b/e)
C-1	2.3	4.80
C-2	2.3	4.82
C-3	2.3	4.78
S-1	2.15	2.12
S-2	2.15	2.13
S-3	2.14	2.12

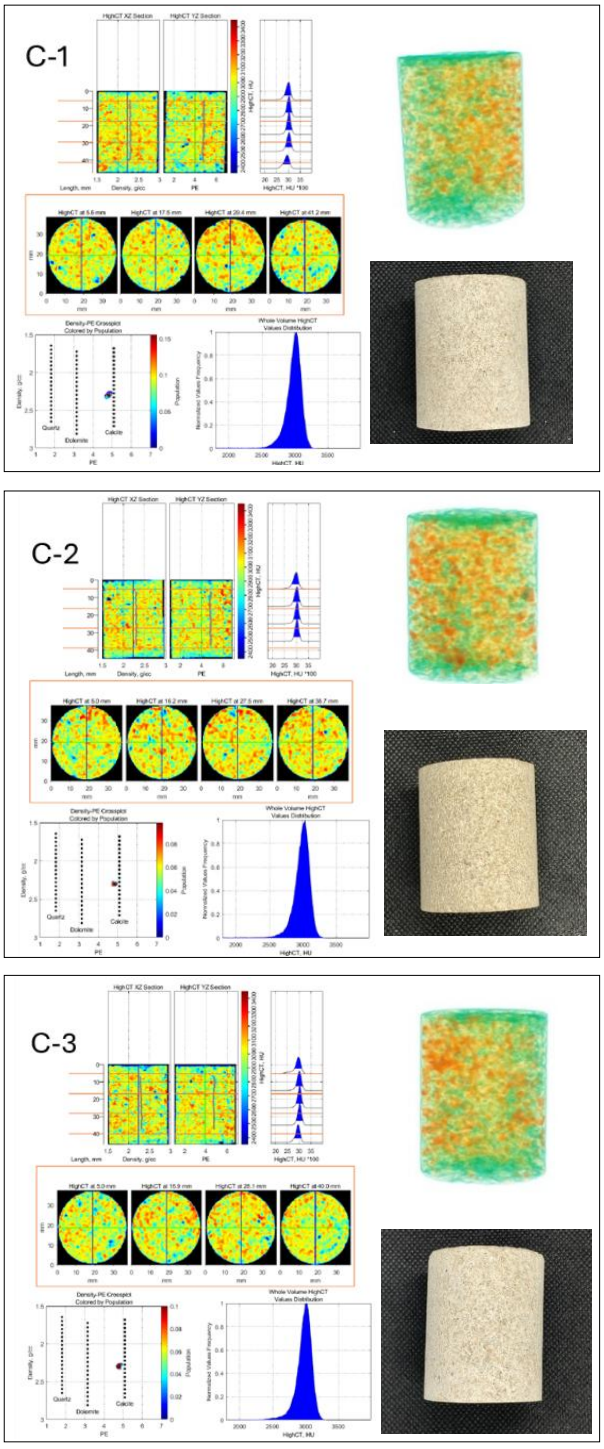

Figure 6. White light photos, color scale 3D CT images and processed RbohB and PE calculated from CT of carbonate samples.

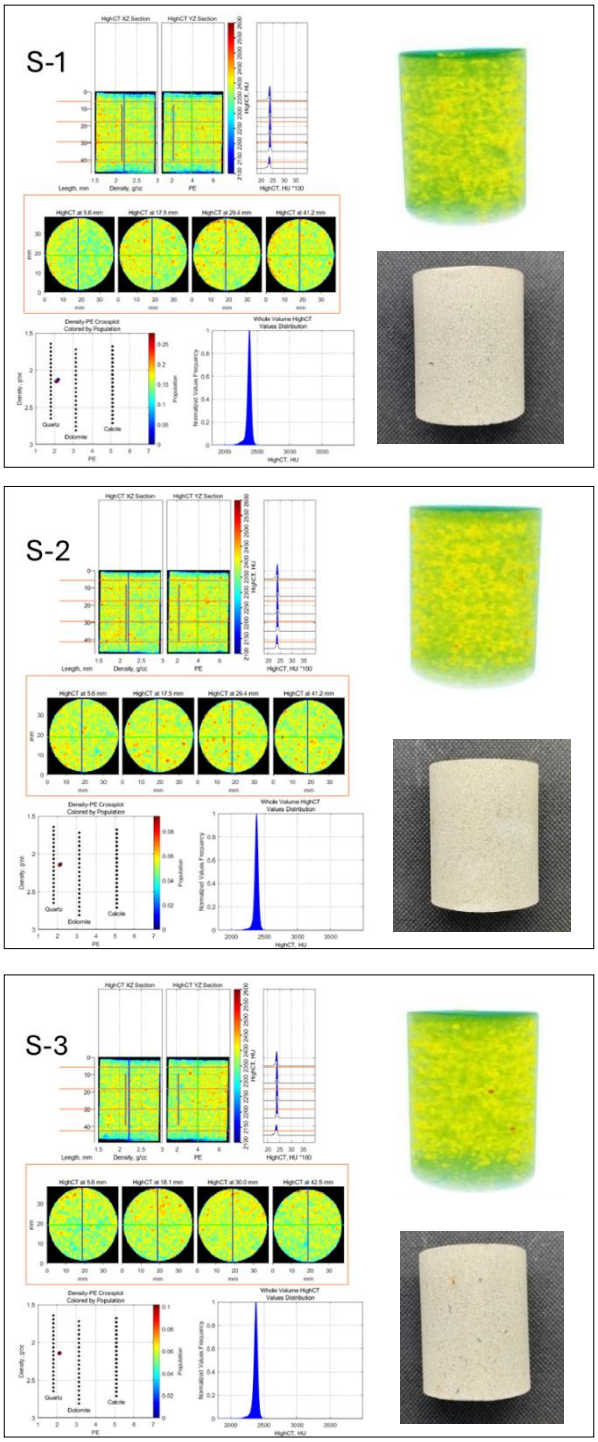

Figure 7. White light photos, color scale 3D CT images and processed RbohB and PE calculated from CT of clastic samples.

4.3 IFT data and analysis

Since reduction of IFT between the displacing oil and initial water is considered as one of the mechanisms to recover part of the S_{wi}, the oil soluble surfactant was mixed with crude oil to test its effect on lowering the IFT. The measured IFT between the crude oil and the brines are 16.75 dyne/cm and 19.94 dyne/cm for the 200 KPPM and 100 KPPM salinity brines, respectively [35]. When adding 1% by volume of the surfactant to the crude oil to make 1% SE oil, the IFT was dropped significantly to 5.9

dyne/cm and 7.49 dyne/cm for the two brines, and further dropped to 1.22 dyne/cm and 3.38 dyne/cm if 2% surfactant is added (Figure 8), i.e., the 2% SE oil reduces the IFT with the 200 KPPM brine by 93% (Table 6).

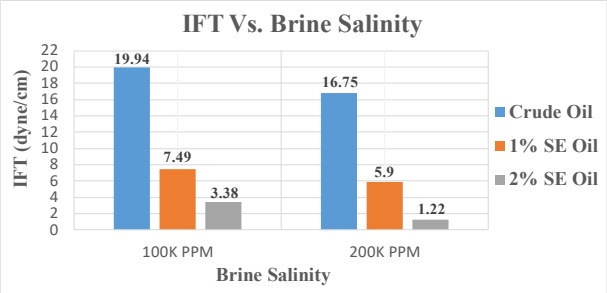

Figure 8. Bar chart plot of IFT results of crude oil, 1% SE oil and 2% SE oil with 200 and 100 KPPM Brines.

Table 6. Effect of surfactant on IFT between oil and salinity at 70°C and 1000 psi

#	Droplet	Brine (KPPM)	IFT (dyne/cm)	IFT Drop (dyne/cm)
1	Crude Oil	100	19.94	Reference
2		200	16.75	
3	1% SE Oil	100	7.49	62%
4		200	5.90	64%
5	2% SE Oil	100	3.38	83%
6		200	1.22	93%

4.4 S_{wi} establishment and aging

Again, to establish S_{wi}, the core samples were fully saturated with the brine (Table 7), which was then displaced by crude oil in a centrifuge at speeds of 6,500 RPM and 3,000 RPM for the carbonate and clastic samples, respectively. Different RPMs were used based on the bond number calculated for each group of samples. Achieved S_{wi} for the carbonate samples ranged from 32.72% to 33.68% and 18.88% to 22.60% for the clastic samples (Table 7). After establishing S_{wi}, all samples were placed in aging cells filled with the crude oil and then placed in an oven for one month at 70°C and 1500 psi for wettability restoration.

Table 7. Summary of primary drainage data after flooding with crude oil using a centrifuge at RPM 1.

ID	Brine salinity	Sat. Brine vol or PV	$Speed_1$	Prod brine	$S_{wi,1}$
	(KPPM)	(cc)	(RPM)	(cc)	(%)
C-1	200	8.18	6500	5.50	32.72
C-2	100	7.47	6500	5.0	33.10
C-3	100	7.84	6500	5.2	33.68
S-1	200	10.48	3000	8.5	18.88
S-2	200	10.52	3000	8.49	19.32
S-3	100	10.21	3000	7.90	22.60

4.5 Recover part of S_{wi} by SE oil displacement

After one month of aging at 70° C and 1500 psi, wettability restoration of the core samples was considered completed. 2% SE oil was then used to displace the aging crude oil and recover part of the S_{wi} using the centrifuge at a higher speed (RPM 2), with respect to RPM 1, enough to produce part of the S_{wi} without risking the samples to break or fail at much higher speed [34]. Consequently, the higher speed RPM 2 used was 8,000 RPM and 4,500 RPM for carbonate and clastic samples, respectively. This would result in partial recovery of the original S_{wi} for both carbonate and clastic samples, due to the lowered IFT of SE oil and water, as well as the higher centrifuge force at a higher RPM [24].

Depending on sample pore volume and S_{wi}, the recovered brine volumes ranged from 0.5 cc to 1.4 cc for the carbonate samples and from 0.6 cc to 0.7 cc for the clastic samples, respectively as shown in Figure 9 and Table 8. It has been noticed that the clastic sample S-3 produced much lower water volume; too small to be neither characterized by the IC nor the titration methodologies. The behavior of this sample could be related to its pore structure as permeability (dominated by the largest connected pore throats) or porosity (pore volume) are not good indicators of S_{wi} distribution.

For the other samples, geochemical analysis can then be conducted by using the produced brine for water salinity, and then water resistivity at a specific reservoir temperature can be determined.

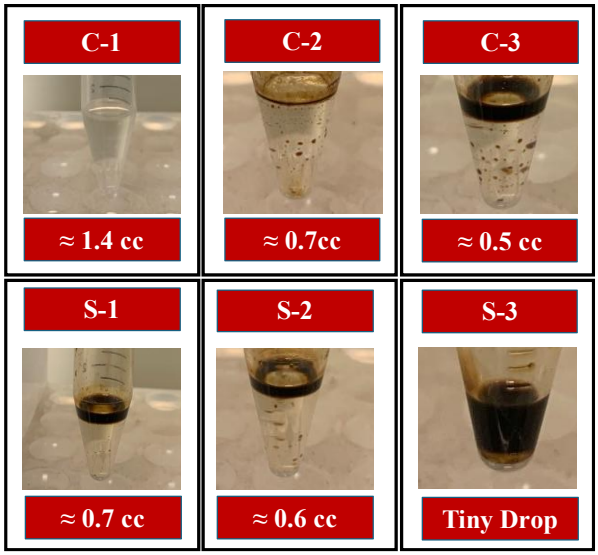

Figure 9. Production of initial water S_{wi} by 2% SE oil displacement at a higher centrifuge RPM.

Table 8. Summary of the secondary drainage data after flooding plugs with 2% SE oil using centrifuge at RPM 2.

Plug ID	Brine salinity	$S_{wi,1}$	$Speed_2$	Prod. brine	$S_{wi,2}$
	(KPPM)	(%)	(RPM)	(cc)	(%)
C-1	200	32.72	8000	1.4	15.60
C-2	100	33.10	8000	0.7	23.74
C-3	100	33.68	8000	0.5	27.30
S-1	200	18.88	4500	0.7	12.20
S-2	200	19.32	4500	0.6	13.61
S-3	100	22.60	4500	≈ 0	22.60

4.6 Geochem analysis of small volume of brine

The recovered part of S_{wi} by using 2% SE oil at a higher centrifuge speed was measured using both IC and titration methods to determine the NaCl concentration on all samples except sample S-3 that didn't produce enough water to be tested, and sample C-3 that was tested using IC method only due to the limited volume remained that was not enough to produce representative results from the titration method. Moreover, two additional brine salinities (150 and 50 KPPM) were prepared and tested using both titration and IC methods to better assess of how representative each methodology is across different concentration ranges.

The following steps were used to characterize the NaCl concentrations from the recovered part of S_{wi};

1. The small volume of brine produced (Table 8) is diluted for geochemical measurement.
2. The measured values are calibrated with measurement technique calibrations; Figure 4 for the titration method and Figure 5 for the IC method.

The results were plotted against the initial measurements of the prepared brines as shown in Figure 10 and 11 for IC and titration analysis, respectively. The good correlations between the measured and prepared illustrate the validity of the method of recovering part of S_{wi} for formation water salinity determination, thus formation water resistivity for improved formation evaluation using the Archie model, Eq 2. Note: (a) three data points are plotted for the 200 KPPM, although they are almost overlapping. (b) the water volume remained for sample C-3 was not enough to be tested using titration method, but the IC method only.

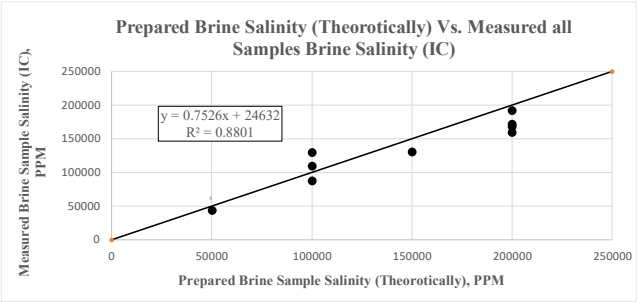

Figure 10. NaCl concentration results of prepared and produced brine samples using IC method.

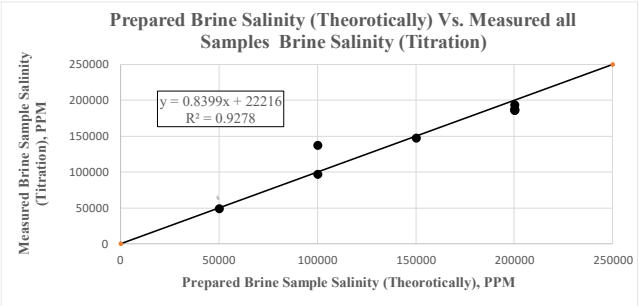

Figure 11. NaCl concentration results of prepared and produced brine samples using titration analysis.

5 Conclusions

A non-destructive method to recover part of initial water saturation (S_{wi}) from oil-based mud drilled core samples is documented and verified. This is possible due to the lowered IFT between the displacing SE oil and displaced S_{wi} water, as well as a higher centrifuge force at a higher RPM.

The success of the above technique depends on initial water volume, V_{wi}, which is a product of sample porosity and S_{wi}. The higher the V_{wi}, the higher the chance to recover a meaningful part of S_{wi}.

Formation water salinity does also have some effects on the amount of S_{wi} brine recovered. The higher the water salinity, the more water recovered. This needs to be tested in more detail in the future.

Because the amount of the recovered S_{wi} water is typically small, geochemical analysis techniques that require sample dilution is an advantage, and measurements calibration is critical for the accuracy of geochemical analysis.

Nomenclature

Abbreviations

API	American petroleum institute
CT	Computed Tomography
IFT	Interfacial tension
OBM	Oil base mud
OOIP	Original oil in place
Poroperm	Porosity & permeability measurement
PPM	Parts per million
K	One thousand
RbohB	Bulk density
RPM	Revolution per minute
Nb	Bond number
SE Oil	Surfactant enhanced oil
XRD	X-ray diffraction
XRF	X-ray fluorescent
SN	Silver nitrate
PC	Potassium Chromate
PE	Photoelectric factor
dr	Drainage
imb	Imbibition

Symbols

%	Percentage
b/e	Barns per electron
g	Gram
K	Air permeability
cc	Cubic centimeter
V_P	Pore volume in cc
°C	Degrees Celsius
ϕ	Porosity
ρ_g	Grain density
Psi	Pound per square inch
mD	Milli darcy
μ	Viscosity
cP	Centipoise
R_w	Formation-water resistivity
S_{wi}	Initial water saturation
V_{wi}	Initial water volume
R_w	Water resistivity
R_t	True resistivity
m	Cementation exponent
n	Saturation exponent
wt%	Weight percent
C_{NaCL}	Sodium Chloride concentration
V_w	Volume of brine sample (mL)
V_{SN}	Volume of Silver Nitrate ($AgNO_3$) used (mL)
N_{SN}	Normality of Silver Nitrate
C_{Cl^-}	Chloride concentration (PPM)
C_{NaCl}	Sodium Chloride concentration (PPM)

References

1. F.I. Stalkup. Displacement of oil by solvent at high water saturation, *SPEJ*, 10(04), 337–348 (1970)
2. B.V. Malozyomov et al., Overview of methods for enhanced oil recovery from conventional and unconventional reservoirs, *Energies* 16, 4907 (2023)
3. A.M. Al-Heeti and O. Al-Fatlawi. A review of historical studies for water saturation determination techniques, *Iraqi Geol. J*. 55, 42–62 (2022)
4. M.H.A. Al-Majid. Petrophysical properties estimation of Euphrates reservoir in Qayyarah oil field using core and well log data, *Iraqi Geol. J*., 186–197 (2021)
5. R. Woodhouse and H. Warner. Sw and hydrocarbon pore volume estimates in shaly sands- routine oil-based-mud core measurements compared with several log analysis models, SPE ATCE, Paper SPE-96618-MS (2005)
6. S. Ma, A. Al-Hajari, D. Kersey, et al. Fit-for-purpose laboratory core analysis and their impact on log processing, SPE-105301, MEOS (2007)
7. G. Archie. The electrical resistivity log as an aid in determining some reservoir characteristics, *Petro Trans of AIME,* v146, p.54-62 (1942)
8. S. Ma, A. Hajari, G. Berberian, et al. Cased-hole reservoir saturation monitoring in mixed salinity environments –a new integrated approach, SPE-92426, MOES (2005)
9. S. Ma, A. Al-Hajari, D. Kersey, et al. Enhanced petrophysics: integration of core and log data for improved reservoir saturation monitoring, SPE-106350, SPEKSA Tech Symp (2006)
10. S. Ma, A. Hajari, O. Kelder, et al. Dynamic petrophysics- applications of time-lapse reservoir monitoring, SPE-95882, ATCE, Dallas (2005)
11. A. Sunbul, S. Ma, A. Hajari, et al. Quantifying remaining oil by use of slim-hole resistivity measurement in mixed salinity environments –a pilot field test, SPE-97489, Int'l IOR Conf. in Asia Pacific, Dec. 5-6, Kuala Lumpur, Malaysia. (2005)
12. S. Ma, H. Pfuzner, A. Hajari, et al. Resolving the mixed salinity challenges with a methodology developed from pulsed neutron capture gamma ray spectral measurements, SPE-170608, SPE ATCE, Amsterdam (2014).
13. S. Ma, N. Al-Musharfi, P. Saldungaray, et al. Formation water salinity from borehole measurements, US Patent 10,208,582, 19 Feb (2019)
14. H. Pfutzner, J. Grau, R. Plasek, et al. Method and apparatus for measuring formation water salinity in a borehole, US Patent 10,247,849, 2 April (2019)
15. I. Mostefai, P. Saldungaray, S. Ma, et al. Formation Chlorine Measurements Using Slimmer Pulsed

Neutron Devices Enhance Reservoir Monitoring, SPE-222204, ADIPEC (2024)

16. P. Zhang, S. Ma, W. Abdallah, et al. Determination of formation water salinity using downhole low frequency electromagnetic measurement and permittivity dispersions based thereon, US Pat 11,796,710, 24 Oct (2023)
17. W. Abdallah, P. Zhang, S. Ma, et al. Quantification of water saturation & salinity using relative permittivity & conductivity measurements, US Patent 12,360,278, 15 July (2025)
18. W. Abdallah, S. Di Santo, A. Solial, et al. Processes for determining formation salinity and saturation, US Patent Application 18/483,736, 10 Oct (2023)
19. M. Al-Hamad, W. Abdallah, S. Ma, et al. Processes for determining formation salinity and identifying oil bearing zones in freshwater pay zones, US Patent Application 18/483,112, 9 Oct (2023)
20. G. Wang, W. Abdallah, S. Ma, et al. Methods for predicting and monitoring downhole salinity variations, US Patent 12,259,517, 25 March (2025)
21. M. Al-Huwaider and S. Ma. System and method for mixed water salinity characterization, US Pat 11,680,484, 20 June (2023)
22. G. Hursan, S. Ma, A. Valori, et al. Study of OBM invasion on NMR logging- mechanisms and applications, SPE-192218, SPE KSA, April (2018)
23. B. Sauerer, M. Al Hamad, S. Ma, et al. Effect of oil-based-mud filtrate on wettability of rock surfaces with different mineralogy and topology, *Journal of Energy & Fuels*, 34(7), June (2020)
24. S.M. Ma and N. Musharfi. Compositions and Methods to Recover Irreducible Water for Enhanced Formation Evaluation, U.S. Patent 10,633,574 B2 (2020).
25. P.L. Gant and W.G. Anderson. Core cleaning for restoration of native wettability, SPE Form. Eval. 3, 131–136 (1988).
26. H. Al Qatari, S.M. Ma, A. Hafez, et al. Core cleaning for wettability restoration- how clean is clean? SPWLA 65th Annual Logging Symp, Paper SPWLA-2024-0011 (2024).
27. S. Mahavadi, M. Al-Hamad, S. Ma, et al. Role of Polar Species in Determining the Interfacial Tension of a Crude Oil/Water System, *J of Energy & Fuels*, 21 June (2022)
28. M. Al-Hamad, S. Mahavadi, S. Ma, et al. Practical model for estimating reservoir crude oil-water interfacial tension, SPWLA-2024-0129, SPWLA 65th Annual symp., 18-22 May (2024)
29. M Al-Hamad, A. AlZoukani, F. Ali, et al. Converting ambient capillary pressure measurements to reservoir stress for improved formation evaluation: a novel approach, paper SCA 2026-012, SCA Annual Symp, Aug 17-21, 2026, Mexico City, Mexico (2026)
30. G. Singer, S. Ma, A. Hafez, et al. Revisiting mercury wetting properties for mercury injection capillary pressure based pore structure characterization, SPE-227589, MEOSGEO, 16-18 Sept, Bahrain (2025)
31. Al-Hamad, A. AlRadhwan, O. Sindt, and S. Ma, 2025. Obtaining grain density of carbonate rocks: core plugs and powder samples, Paper SPE-227052, MEOSGEO, 16-18 Sept, Bahrain
32. S. Al-Ofi, S. Ma, and G. Jin, 2023. Resolving Challenges in Analyzing Iron-Rich Samples by X-Ray Diffraction, The 36th International Symposium of the Society of Core Analysts, Abu Dhabi, 9-12 Oct
33. W. Guo, S. Ma, and J. Kharrazi, 2026. Petrography-guided mineral identification and quantification- user perspectives based on a multi-lab comparative study of XRD, XRF, and FTIR, paper SCA 2026-002, SCA 2026 Annual Symposium, August 17-21, 2026, Mexico City, Mexico.
34. S. Ma, A. Belowi, F. Pairoys, et al. Quality assurance of carbonate rock special core analysis- lesson learnt from a multi-year research, IPTC-16768, Beijing, China, 26-28 March (2013)
35. B. Sauerer, M. Al-Hamad, S. Ma, et al. Effect of formation water salinity on interfacial tension of reservoir fluids, *J of Petroleum Science and Engineering*, v.204, Sept (2021)